

## Tsunami Bore Overtopping Of Coastal Structures

Esteban, Miguel; Takabatake, Tomoyuki; Glasbergen, Toni; Hofland, Bas; Nishida, Yuta; Nishiazaki, Shinsaku; Stolle, Jacob; Nistor, Ioan; Takagi, Hiroshi; Bricker, Jeremy

**Publication date**

2018

**Document Version**

Final published version

**Published in**

Proceedings of the 7th International Conference on the Application of Physical Modelling in Coastal and Port Engineering and Science (Coastlab18)

**Citation (APA)**

Esteban, M., Takabatake, T., Glasbergen, T., Hofland, B., Nishida, Y., Nishiazaki, S., Stolle, J., Nistor, I., Takagi, H., Bricker, J., & Shibayama, T. (2018). Tsunami Bore Overtopping Of Coastal Structures. In *Proceedings of the 7th International Conference on the Application of Physical Modelling in Coastal and Port Engineering and Science (Coastlab18): Santander, Spain, May 22-26, 2018*

**Important note**

To cite this publication, please use the final published version (if applicable).  
Please check the document version above.

**Copyright**

Other than for strictly personal use, it is not permitted to download, forward or distribute the text or part of it, without the consent of the author(s) and/or copyright holder(s), unless the work is under an open content license such as Creative Commons.

**Takedown policy**

Please contact us and provide details if you believe this document breaches copyrights.  
We will remove access to the work immediately and investigate your claim.

## **TSUNAMI BORE OVERTOPPING OF COASTAL STRUCTURES**

MIGUEL ESTEBAN<sup>1</sup>, TOMOYUKI TAKABATAKE<sup>2</sup>, TONI GLASBERGEN<sup>3</sup>, BAS HOFLAND<sup>4</sup>, YUTA NISHIDA<sup>5</sup>, SHINSAKU NISHIAZAKI<sup>6</sup>, JACOB STOLLE<sup>7</sup>, IOAN NISTOR<sup>8</sup>, HIROSHI TAKAGI<sup>9</sup>, JEREMY BRICKER<sup>10</sup>, TOMOYA SHIBAYAMA<sup>11</sup>

*1 The University of Tokyo, Japan, esteban.fagan@gmail.com*

*2 Waseda University, Japan, tomoyuki.taka.8821@gmail.com*

*3 Delft University of Technology, The Netherlands, toniglasbergen92@gmail.com*

*4 Delft University of Technology, The Netherlands, b.hofland@tudelft.nl*

*5 Waseda University, Japan, yuta325@ruri.waseda.jp*

*6 Waseda University, Japan, shinsaku-nisshi@fuji.waseda.jp*

*7 University of Ottawa, Canada, jstol065@uottawa.ca*

*8 University of Ottawa, Canada, inistor@uottawa.ca*

*9 Tokyo Institute of Technology, Japan, takagi@ide.titech.ac.jp*

*10 Delft University of Technology, The Netherlands, J.D.Bricker@tudelft.nl*

*11 Waseda University, Japan, shibayama@waseda.jp*

### **ABSTRACT**

In the aftermath of the *2011 Tohoku Earthquake and Tsunami* Japanese tsunami protection philosophy now dictates that coastal defences should prevent the land that they protect from being flooded under a Level 1 event (with a return period in the order of about 100 years). To ascertain the overtopping mechanism and leeward inundation heights of tsunamis as they hit coastal structures, the authors conducted physical experiments using a dam-break mechanism, which could generate bores that overtopped different types of structures. Three different types of structures were considered, namely a wall of “infinite” height, a coastal dyke, and a vertical tsunami wall. The results show that the velocity of the tsunami bore is crucial in determining whether the structure will be overtopped or not, and thus it is imperative to move away from only considering the tsunami inundation height at the beach.

**KEYWORDS:** tsunami bores, overtopping, dam break, coastal dykes, laboratory experiments

### **1 INTRODUCTION**

The *2011 Tohoku Earthquake and Tsunami* overcame coastal defenses and flooded much of the northeast coast of Japan, and is considered to be one of the most severe events to have affected Japan since historical records began. The tsunami went on to destroy much of the coastal structure and settlements, with maximum inundation and run-up heights of between 10 to 40 m along the Tohoku coastline (Mori et al., 2011). The 2011 event is currently considered to be a Level 2 tsunami, with a return period greater than 1 in 1000 years (Shibayama et al., 2013). Essentially, following the 2011 event the Japanese coastal engineering community has classified tsunami events into two different levels, according to their level of severity and intensity. Level 1 events correspond to return periods of the order of 100+ years, resulting in inundation levels typically around 7 to 10 m. Level 2 events would have return periods of a few hundred to a few thousand years, and the inundation heights would be much larger, over 10 m (Shibayama et al., 2013). “Hard measures”, such as breakwaters or coastal protection dykes, should be strong enough to protect against the loss of life and property against a Level

1 event. However, it is accepted that coastal dykes and other types of countermeasures would be overtopped by Level 2 events, though evacuation procedures and shelters should be designed with such a tsunami in mind. Nevertheless, hard measures would also play a secondary role in delaying the incoming wave and giving residents more time to evacuate (Tomita et al., 2012), highlighting the importance of correctly designing such structures to help mitigate (or completely eliminate) the loss of life.

A number of different field surveys reports have highlighted a variety of failure mechanisms of coastal structures (Mikami et al., 2012, 2014, Kato et al., 2012, Esteban et al., 2014, Jayaratne et al., 2016), which typically involved toe scour at the land side of the structure (see Fig. 1). Normal breakwaters are basically designed to reflect wind waves, and thus in general the reduction of the tsunami impact due to these structures should also not be overestimated (Takagi and Bricker, 2014). Prior to the 2011 event, a number of laboratory experiments had been performed regarding how to design dykes and vertical structures against wind waves (Goda, 1985, Tanimoto et al., 1996, Esteban et al., 2007). Tanimoto et al. (1984), Ikeno et al. (2001, 2003), and Mizutani and Imamura (2000) all performed experiments to calculate the wave pressure of a bore on coastal structures. Esteban et al. (Esteban et al., 2008, 2009, 2012) calculated the deformation of the rubble mound foundation and behavior of the armour of composite breakwaters against different types of solitary waves and bore-like conditions. However, the use of solitary waves in tsunami modelling has been called into question, due to the relatively short distance between the source region and coast when compared to the distance in which a soliton forms (Madsen, 2008). As such, the use of solitary waves can only consider the incipient motion of the tsunami wave (Gosebert, 2013). A number of other researchers (Sakakiyama, 2012, Hanzawa et al., 2012, Kato et al., 2012) have proposed methods to design the armour of breakwaters against tsunami attack, focusing on the current velocity and the overtopping effect. It is evident that beach bathymetry, onshore coastal topography, coastal geomorphology, coastal structure geometry, and (tsunami) wave conditions, all influence the failure modes and mechanisms of coastal structures (Jayaratne et al., 2016). Computer simulations have shown how, despite failing, these types of structures can be effective in mitigating tsunami damage (Nandasena et al., 2012, Stansby et al., 2008, Hunt-Raby et al., 2011) and reducing the number of casualties (Ratnayakage et al., 2017, Latcharote et al., 2016, Okumura et al., 2017).

However, despite the wealth of research conducted on the structural behavior of structures under a bore attack, to the authors' knowledge comparatively little experimental work has been done on the overtopping nature of the tsunamis over coastal dykes. The construction of coastal dykes can provide extra time for local residents to evacuate, without the need to construct them high enough that they would become economically unfeasible (Okumura et al., 2017). Several researchers have studied evacuation in specific locations, such as Kamakura City (Japan), highlighting the importance of evacuation procedures and communication to improve the evacuation of local residents and tourists in the case of a tsunami event (San Carlos-Arce et al. 2017, Takabatake et al., 2017).

Hence, the authors set out to investigate the characteristics of overtopping flows that result from a variety of different incident bore-type tsunami conditions. Laboratory experiments were carried out using a dam-break generation mechanism, with a bathymetry that simulates a typical beach profile along the Japanese coast, protected by various types of structures.



**Fig. 1. Failure of coastal dykes along the Tohoku coastline. In many places the dykes were completely breached (left), or suffered heavy scour (right).**

## 2 METHODOLOGY AND APPARATUS

Laboratory experiments using a dam break generation mechanism were performed in a wave flume (dimensions 14 m × 0.41 m × 0.6 m) at Waseda University, Tokyo, Japan. Froude scaling of 1:50 was used, with a schematic representation of the experimental apparatus being shown in Figure 2. On one side of the tank, a dam break generation mechanism was constructed, operated by a system of pulleys that were attached to a heavy weight (see Figure 3, left). The release of the weight lifted the gate, and, as this weight was kept constant, the speed at which the gate was raised was similar for all of the experiments. The reservoir was 4.5 m long in order to ensure that a long bore was generated (between 18.9 and 37.8 m<sup>3</sup> of water were released in every experiment, depending on the experimental condition).

The “wave half-period”,  $T/2$ , was estimated from the profile of the bore when no structure was present in the tank. For the cases when the amount of water in the tank was limited, this value could be calculated precisely ( $T/2 = 10.6$  s for  $h = 30$  cm and  $d = 0$  cm, for example), though as the amount of the water behind the reservoir increased the reflected wave arrived at the wave gauge before a complete wave cycle could be estimated (thus, it was only possible to conclude that  $T/2 > 16.1$  for  $h = 60$  cm and  $d = 0$  cm). A total matrix of 12 experimental conditions were carried out, for  $d = 30, 40, 50,$  and  $60$  cm, and  $h = 0, 10$  and  $20$  cm (Table 1).

A 20 cm high false metallic bed was placed in front of the gate, with the beginning of the 1:10 sloping section starting 5 cm from the edge of the gate. The main testing section was located at the other side of the tank, where three different coastal structures were tested: a high tsunami wall (39 cm high, to attempt to reproduce the effect of a wall of “infinite height”), a coastal dyke, and a low tsunami wall. The high tsunami wall was made using an acrylic panel; the low tsunami wall was constructed using a concrete block 15 cm high and 10 cm wide; and the dyke was made using a combination of acrylic panels and a hollow metallic structure, (9.5 cm high, 26 cm long across the base and 6 cm wide at the top), see Figure 4. All structures were fixed to the sides of the tank using silicon and were completely sealed.

A number of wave gauges (WG) and velocity meters (VM) were placed throughout the tank, as shown in Figures 2 and 4. Table 1 shows a summary of the instrumentation positions that were used. The velocity meters were placed at the top of the structure and 15 cm behind it, to measure the overtopping conditions. The experiments were also repeated without any structures present in the tank, to evaluate the hydrodynamic conditions of the wave. The velocity meters (KENEK VMT2-200-04P, 04PL) that were used in the experiment were electromagnetic current meters (ECMs). The maximum range of measurement was 200 cm/s, and a low pass filter of 20 Hz was applied after the data acquisition. Due to cavitation around the probe head and air bubbles entrained within the turbulent bore, the complete velocity profile could not be captured for the entire length of the experiments, and thus the bore front velocities were actually calculated from more reliable measured data obtained from the wave gauges (WGs), as discussed later. The instruments were connected to a data logging system (KENEK ADS2016), which was itself connected to a PC. The sampling frequency of all the measurements was 200 Hz. A Nikon D5200 camera was mounted on a tripod to record the experiments, which were later analyzed frame-by-frame using computer software.

At the beginning of each experiment the tank was drained and filled to a specified height with water using pumps (both for the water in the reservoir and in front of the gate). Wet bed conditions were used for all of the experiments, as the false bed was not dried between tests. To ensure replicability, certain experimental conditions were repeated several times, as will be explained later.

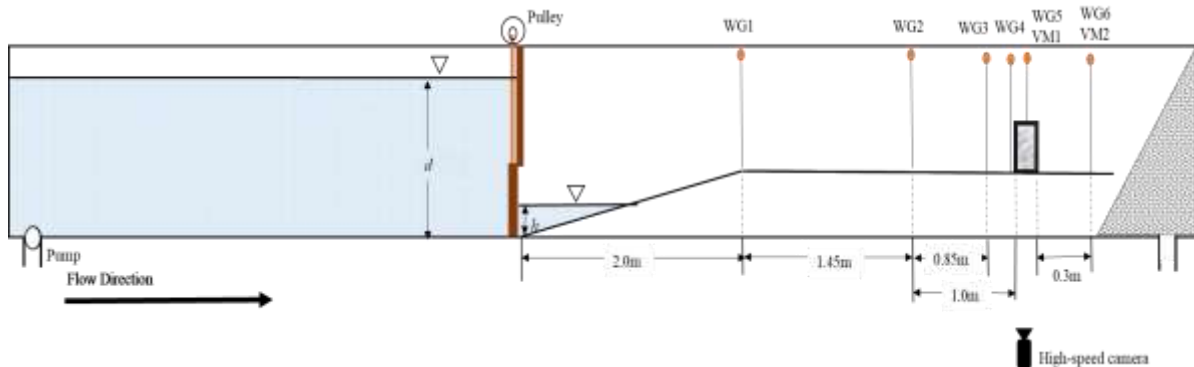


Figure 2. Schematic of the wave flume and instrumentation (not to scale).



Figure 3. Experimental Apparatus. Left: Weight system to release the gate. Right: wave gauge and velocity meters

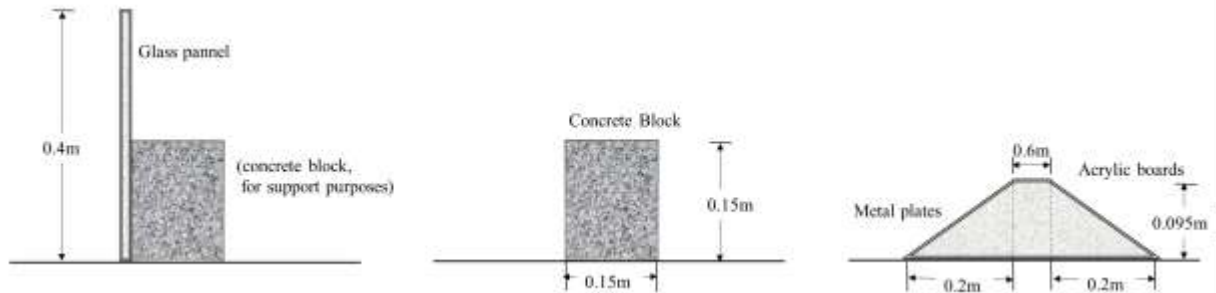


Figure 4. Schematic representation of the coastal structures tested (not to scale). From left to right, "high vertical wall", "low vertical wall" and dyke.

Table 1. Summary of experimental conditions and testing (the table will be referred to throughout the results section, and some definitions appear in diagrams within that section). Numbers in bold italics shows the experimental conditions that were repeated 5 times

| Structure Type |          | No Structure |             | High Vertical Wall (Non-Overtopped) |      | Low Vertical Wall |              |             | Dyke         |              |             |
|----------------|----------|--------------|-------------|-------------------------------------|------|-------------------|--------------|-------------|--------------|--------------|-------------|
| $d$ (cm)       | $h$ (cm) | $H_i$ (cm)   | $V_i$ (m/s) | $H_p$ (cm)                          |      | $H_f$ (cm)        | $H_o$ (cm)   | $H_b$ (cm)  | $H_f$ (cm)   | $H_o$ (cm)   | $H_b$ (cm)  |
|                |          | WG5          | WG2-4       | WG3                                 | WG4  | WG3               | WG5          | WG6         | WG3          | WG5          | WG6         |
| 30             | 0        | 3.42         | 1.24        | 8.24                                | 6.8  | 8.57              | 0            | 0           | 8.06         | 0.41         | 1.43        |
|                | 10       | 3.67         | 1.15        | 7.79                                | 6.81 | 7.15              | 0            | 0.02        | 8.57         | 0            | 0.61        |
|                | 20       | 3.73         | 0.88        | 8.2                                 | 6.52 | 7.49              | 0            | 0.02        | 8.7          | 0.04         | 0.12        |
| 40             | 0        | 5.49         | 1.68        | 16.15                               | 13.1 | 15.21             | 0.9          | 1.48        | 13.73        | 5.55         | 4           |
|                | 10       | 5.64         | 1.37        | 14.59                               | 11.7 | 14.46             | 0.21         | 1.41        | 13.39        | 4.41         | 2.4         |
|                | 20       | 5.64         | 1.79        | 15.41                               | 12.9 | 14.85             | 0.57         | 1.62        | 13.58        | 3.89         | 2.58        |
| 50             | 0        | 8.59         | 2.12        | 24.3                                | 20.6 | <b>21.04</b>      | <b>10.76</b> | <b>5.31</b> | <b>17.61</b> | <b>11.35</b> | <b>7.56</b> |
|                | 10       | 7.79         | 1.92        | 22.38                               | 18.2 | 19.28             | 4.92         | 3.26        | 17.11        | 9.22         | 6.88        |
|                | 20       | 8.32         | 1.66        | 21.41                               | 19.7 | 20.16             | 5.31         | 4.3         | 17.97        | 10.45        | 7.38        |
| 60             | 0        | 12.17        | 2.59        | 33.69                               | >30  | 27.55             | 16.33        | 9.45        | 20.32        | 16           | 9.92        |
|                | 10       | 10.74        | 2.43        | 28.61                               | >30  | 24.35             | 11.11        | 6.95        | 20.36        | 13.16        | 8.95        |
|                | 20       | 10.27        | 2.7         | 28.63                               | 24.2 | 24.17             | 12.38        | 6.88        | 20.89        | 13.48        | 10.12       |

### 3 RESULTS

#### 3.1 Experimental Repeatability

To test whether the experiments were consistent and reproducible between tests, the “low tsunami wall” and “dyke” structure experiments with  $d = 50$  cm and  $h = 0$  cm were repeated five times (Table 1). The standard deviation of the profile of the wave surface at each gauge was low, with a maximum error of 11.41% and 8.47% for WG5 and WG6, respectively (less than 2% for WG1 and WG3). However, the velocity measurements were less consistent, as indicated earlier, and should be treated with caution. For VM1, there was an error of 6.21%, though this climbed to 67.15% for the case of VM2. The errors for the dyke experiments were similar for the case of WG1 and WG3, and slightly lower for WG5 and WG6 (under 6.5%), and the velocity metres (9.99% and 45.14% for VM1 and VM2, respectively).

#### 3.2 Bore Wave Profile

For some of the experiments, the velocity of the incident bores exceeded the capabilities of the velocity metres (200 cm/s), and many data points were lost due to air entrapment behind the probes. To overcome this problem, the bore front velocity was used to approximate the maximum kinetic energy of the wave, as it appears that the flow velocity at the tip of a bore is approximately equal to the bore front velocity (see Dressler, 1954, Estrade and Martinot, 1964, Chanson, 2006). The bore front velocity was calculated by computing the time for the bore tip to travel between WG2 and WG4—situated exactly 1.0 m apart—for the case when no structure was present in the tank (Sett Table 1). The incident wave height ( $H_i$ ) was taken as the maximum height of the wave as it traversed WG5, as this wave gauge was situated where the structures would later be placed.

When there were structures in the tank the incident bore would only overtop them if there was sufficient energy present in it. To analyse the overtopping effect, a number of parameters were defined, as shown in Figure 5 and Table 1.  $H_f$ ,  $H_o$ , and  $H_b$  are the maximum values of the water surface elevation of the bore as it impacts, overtops, and continues to run behind the low wall or the dyke. For the case of a non overtopping structure the key parameter that was introduced was  $H_{ff}$ , which is the maximum value of the surface profile of the wave as it impacts the high seawall, which is given by WG4). The time history of water elevation for each of these wave gauges is given in Figure 6, for the case of the low tsunami wall,  $h = 0$  cm and  $d = 30, 40, 50,$  and  $60$  cm, with Figure 7 showing the corresponding photograph frames for each of the cases shown in Figure 6. Note that Figure 7 also shows the water elevation profiles for the dykes that were tested, in order to be able to compare them to the low tsunami wall.

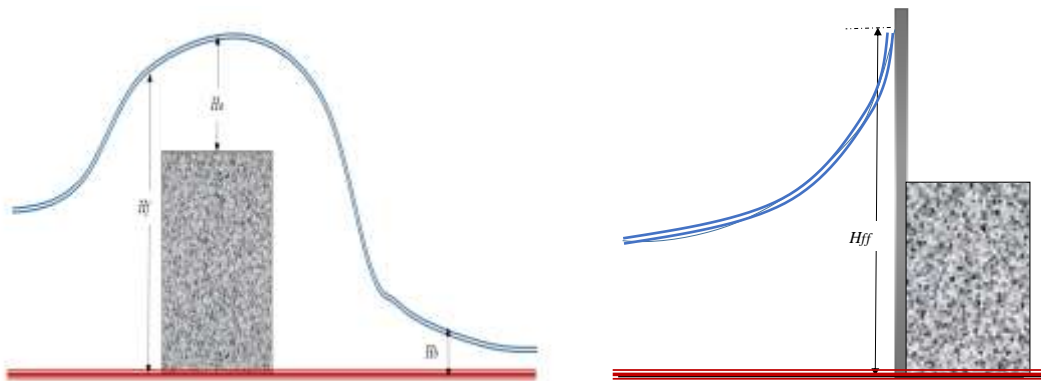


**Figure 5. Left: Wave parameters for overtopping structure ( $H_f$ ,  $H_o$ , and  $H_b$  are the maximum values of the surface profile of the wave as it impacts, overtops and continues to run behind the structure, given by WG3, WG5, and WG6, respectively). Right: Incident wave parameters for non-overtopping structure ( $H_{ff}$  is the maximum values of the surface profile of the wave as it impacts the high seawall, as given by WG4)**

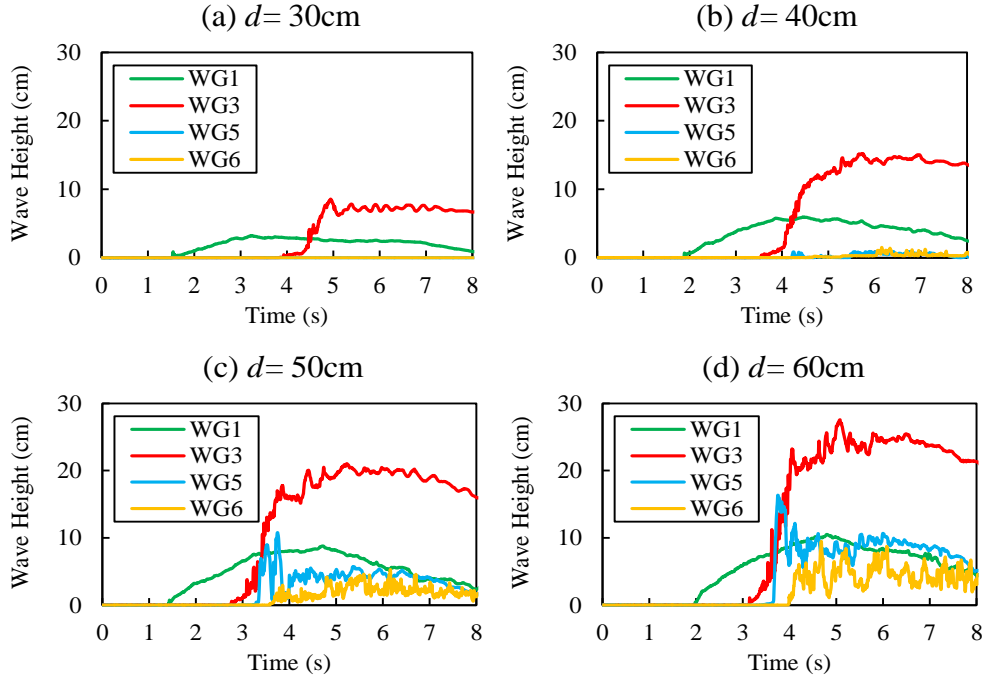


Figure 6. Time history of water elevation of representative bores attacking the low vertical wall. All cases shown are for no water in front of the gate ( $h = 0$  cm), and depths of water in the tank  $d = 30, 40, 50$  and  $60$  cm

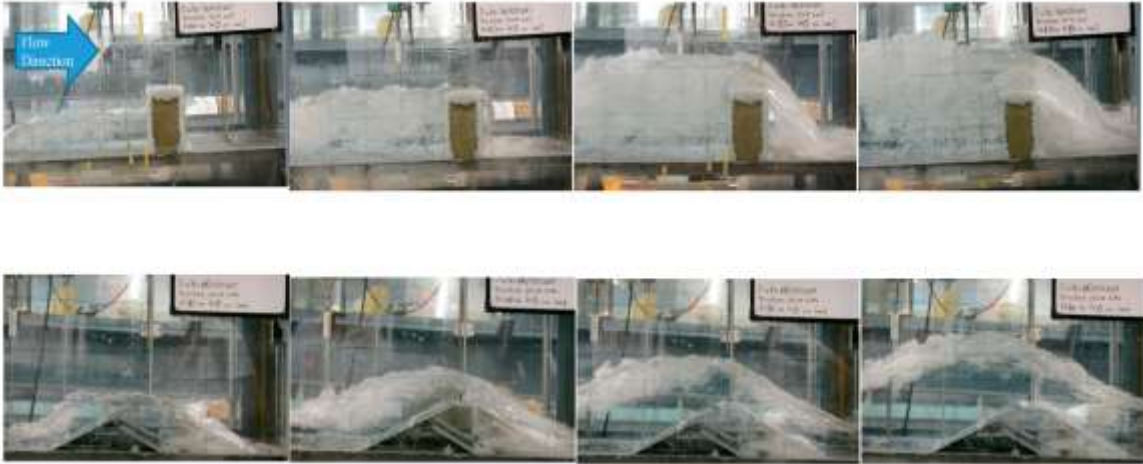


Figure 7. Comparison of different overflowing patterns for various types of incident bores, for the low tsunami wall and dyke structure. All photographs are for the  $h = 0$  cm cases, and  $d = 30, 40, 50$  and  $60$  cm (left to right)

### 3.3 Inundation height seaward and landward of the structure

The energy of the incoming tsunami bore as it traverses WG5 for the case when no structure is present is given by the following equation:

$$E_i = \frac{V_i^2}{2g} + H_i \quad (1)$$

where  $E_i$  is the specific energy head,  $V_i$  is the maximum incident bore front velocity in front of the structure,  $g$  is the acceleration due to gravity, and  $H_i$  is the maximum incident bore wave depth.

For the high wall case Figure 8 shows the relationship between  $H_{ff}$  and  $H_i$ ,  $V_i/2g$  (velocity head), and  $E_i$ , respectively (except the results of  $d = 60, h = 0$  and  $d = 60, h = 10$ , as  $H_{ff}$  exceeded the capability of WG4 (30

cm) in these cases), where  $H_{ff}$  is higher than  $H_i$  in all of the cases. Hence, it is possible for the tsunami to overtop the structure even if the tsunami height is lower than it, if it has a high kinetic energy.

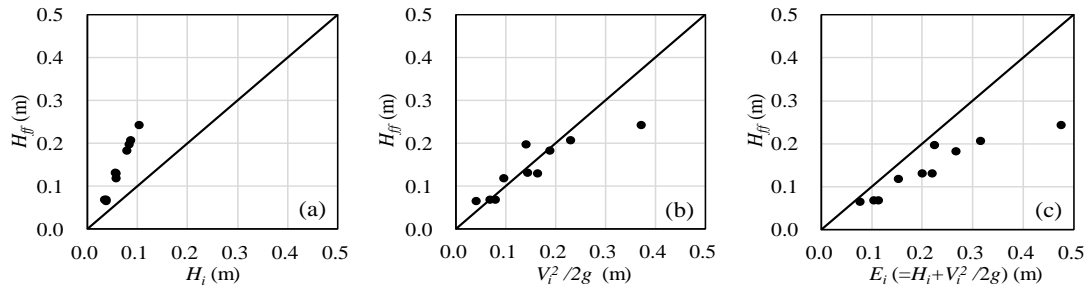


**Figure 8. Relationship between the wave depth in front of the high wall ( $H_{ff}$ ) and the incident wave height ( $H_i$ ), velocity head ( $V_i^2/2g$ ), and the specific energy ( $H_i + V_i^2/2g$ ).**

According to the definition of the Froude number ( $Fr^2 = u^2/gh = V_i^2/gH_i$ ), and assuming that the energy head of the incoming flow,  $E_i$ , will equal the water level at the wall, the ratio between the wall height that is required to completely block a tsunami,  $h_{w0}$  and the undisturbed bore height,  $H_i$ , could be estimated as:

$$h_{w0}/H_i = (Fr^2/2 + 1) \tag{2}$$

This seems to give a crude, but safe upper bound estimate for the required wall height. The measured water depths in front of the structure are compared to eq. (2) in Figure 9 below. For lower walls (in terms of  $h_w/E_i$ ), the measured water depths in front of the wall are somewhat lower than for the high wall—up to roughly 20% to 30%—as can be seen in Figure 10 below.

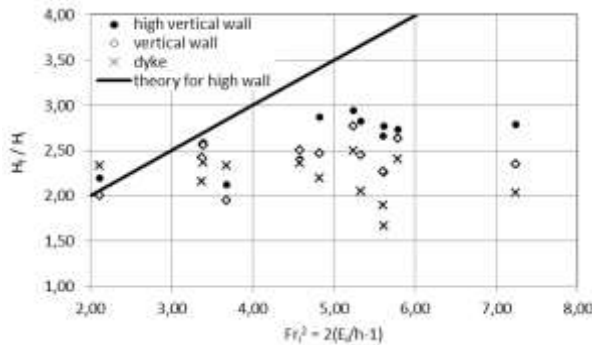


**Figure 9. Water depth in front of wall compared to eq. (2).**

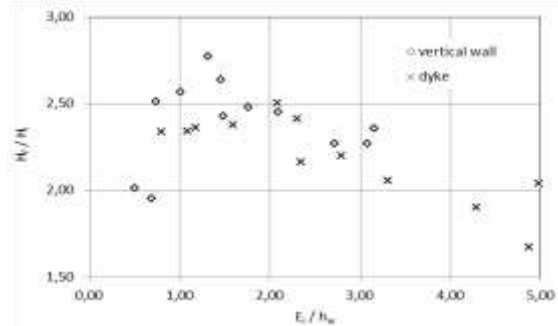


**Figure 10. Water depth in front of wall as function of energy head – wall height ratio.**

To understand the inundation that can be caused by a tsunami overtopping a dyke the ratio  $H_b/H_i$  needs to be considered (see Figure 9), which can be given as a function of  $E_i$ . For the case of low  $H_i$ ,  $V_i^2/2g$ , and  $E_i$ , the wave did not substantially overtop the structure, and this was capable of completely stopping the wave. As those values increased, the ratio  $H_b/H_i$  also increased, and the wave started to overtop the structure. Once these values became high enough the bore bypassed the structure, without suffering any significant influence from the obstruction, clearly showing the importance of considering the incoming wave velocity when determining whether a structure will be overtopped or not. To further clarify the influence of the structure, these values were divided by the height of structure ( $H_w$ ), as shown in Figure 10.



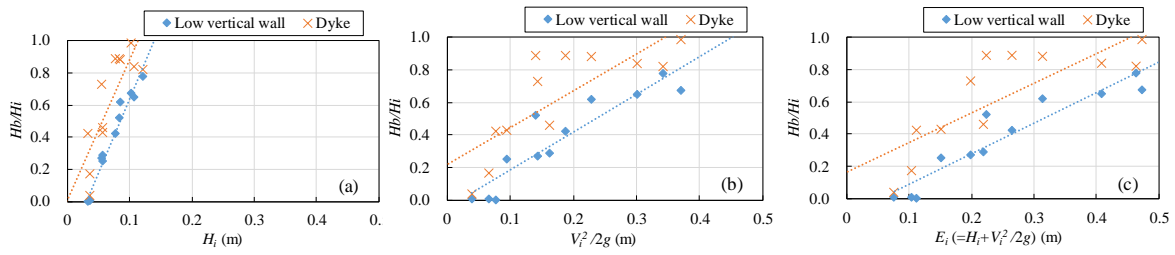


**Figure 9.** Relationship between the ratio of wave depth after the wall ( $H_b$ ) and the incident wave height ( $H_i$ ), and the incident wave height ( $H_i$ ), velocity head ( $V_i^2/2g$ ), and the specific energy ( $H_i + V_i^2/2g$ ).

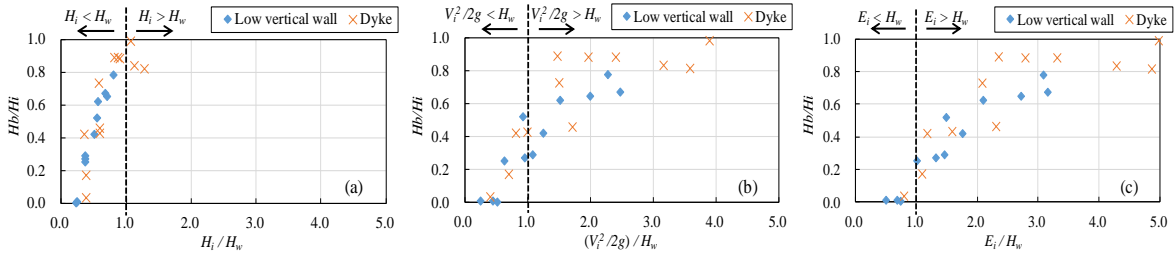


**Figure 10.** Relationship between the ratio of wave depth after the wall ( $H_b$ ) and the incident wave height ( $H_i$ ), and the dimensionless values  $H_i/H_w$ ,  $(V_i^2/2g)/H_w$ , and  $E_i/H_w$ .

It is still an open question to which extent the generated bores resemble real tsunamis. In recent work that followed these lab experiments it seems that the kinematic dimensions (Froude numbers) of the initial bore front resemble those of real life tsunamis at the coastline (Glasbergen, 2018). In those simulations, hundreds of metres inland the flow velocities decreased, compared to the velocities at the shore line. These real life kinematics were estimated using a numerical model (SWASH), which calculates the tsunami evolution from the source region to the maximum run-up point.

Evidence from the field indicates that not all structures were significantly overtopped, and how in areas where the bore might not have possessed enough energy only minor flooding was recorded behind the structures. One such case can be seen for example in Fudai, where the floodgates and dykes were effective at dissipating the tsunami's energy, despite them being partially overtopped (Fig. 11, left). However, when the defences were not high enough and the tsunami carried enough energy they were overtopped and the wave went on to destroy the town behind them (such as at Taro, for example, Fig. 11, right).



**Figure 11.** Left: dyke and floodgates at Fudai, which successfully stopped the force of the tsunami, despite being partially overtopped (inundation marks of ~20m in front of the structure). Right: coastal defences at Taro were overtopping by the tsunami, which went on to completely destroy the town behind them.

## 4 CONCLUSIONS

A wide range of laboratory experiments using a dam-break mechanism were conducted on three types of coastal structures, with the aim of understanding how the overtopping processes affects the inundation height behind them. Through these experiments the authors proved that the amount of energy in the approaching bore is critical in determining whether the structure will be overtopped or not, which ties in well with real life examples of the overtopping of coastal defences, which shows that some structures were overtopped and others were not. This highlights the need to move away from only considering the inundation height of the tsunami wave at the beach, and also consider its velocity.

Allowing for reduced flooding would be needed to improve the effectiveness of the soft engineering methods, which are of paramount importance to save lives during a tsunami event. Therefore, the presence of such structures can clearly improve the resilience of coastal communities against disasters, which is of paramount importance to make them sustainable in the long run, particularly in areas frequently affected by tsunamis, such as the Tohoku coastline (Esteban et al., 2015).

It is important to note that for the case of the *2011 Tohoku Earthquake Tsunami* there is considerable evidence indicating that structures were quite effective at mitigating tsunami damage, and thus the bores might not have had as much energy as some of those that were modelled in the present work. Thus, it is important that tsunami propagation from generation to overtopping is further clarified, for example by looking at issues of energy dissipation at the “beach” in front of the structures. This can be done by modifying the beach width, geometry, and roughness, and the authors will endeavour to continue to work on such issues in the future.

## ACKNOWLEDGEMENT

The laboratory experiments detailed in the present work were financially supported by the Strategic Research Foundation Grant-aided Project for Private Universities from the Japanese Ministry of Education, Culture, Sports, Science and Technology to Waseda University (No. S1311028) (Tomoya Shibayama). TU Delft participation was funded by the Delta Infrastructure and Mobility Initiative [DIMI]. The authors would also like to appreciate the support of the Japanese Ministry of Education (Mombukagakusho), and the Graduate Program on Sustainability Science, Global Leadership Initiative (GPSS-GLI).

## REFERENCES

- Chanson, H., 2006. Analytical solutions of laminar and turbulent dam break wave. In *Proceedings of the International Conference on Fluvial Hydraulics*, Lisbon, Portugal, 6–8 September 2006; Ferreira, R.M.L., Alves, E.C.T.L., Leal, J.G.A.B., Cardoso, A.H., Eds.; Taylor & Francis Groupe: London, UK, 2006; Volume 1, pp. 465–474, ISBN:0-415-40815-6.
- Dressler, R.F., 1954. Comparison of theories and experiments for hydraulic dam-break wave. *Int. Assoc. Sci. Hydrol.* 38, 319–328.
- Esteban, M.; Takagi, H.; Shibayama, T., 2007. Improvement in calculation of resistance force on caisson sliding due to tilting. *Coast. Eng. J.* 49, 417–441.
- Esteban, M.; Danh Thao, N.; Takagi, H.; Shibayama, T., 2008. Laboratory experiments on the sliding failure of a caisson breakwater subjected to solitary wave attack. In *Proceedings of the Eighth ISOPE Pacific/Asia Offshore Mechanics Symposium*, Bangkok, Thailand, 10–14 November 2008.
- Esteban, M.; Danh Thao, N.; Takagi, H.; Shibayama, T., 2009. Pressure exerted by a solitary wave on the rubble mound foundation of an armoured caisson breakwater. In *Proceedings of the 19th International Offshore and Polar Engineering Conference*, Osaka, Japan, 21–26 June 2009.
- Esteban, M.; Morikubo, I.; Shibayama, T.; Aranguiz Muñoz, R.; Mikami, T.; Danh Thao, N.; Ohira, K.; Ohtani, A., 2012. Stability of rubble mound breakwaters against solitary waves. In *Proceedings of the 33rd International Conference on Coastal Engineering*, Santander, Spain, 1–6 July 2012.
- Esteban, M.; Jayaratne, R.; Mikami, T.; Morikubo, I.; Shibayama, T.; Danh Thao, N.; Ohira, K.; Ohtani, A.; Mizuno, Y.; Kinoshita, M.; et al., 2014. Stability of breakwater armour units against tsunami attack. *J. Waterw. Ports Coast. Ocean Eng.* 140, 188–198.
- Esteban, M., Onuki, M., Ikeda, I and Akiyama, T. 2015. Reconstruction Following the 2011 Tohoku Earthquake Tsunami: Case Study of Otsuchi Town in Iwate Prefecture, Japan” in *Handbook of Coastal Disaster Mitigation for Engineers and Planners*. Esteban, M., Takagi, H. and Shibayama, T. (eds.). Butterworth-Heinemann (Elsevier), Oxford, UK
- Estrade, J.; Martinot, A., 1964. Ecoulement consecutif a la suppression dun barrage dans un canal horizontal de section rectangulaire. *Comptes Rendus Hebdomadaires des Seances de L’Academie Des Sciences.* 1964, 259, 4502. (In French)
- Glasbergen, T. Parameters of incoming tsunami bores for the design of coastal defence structures with numerical model SWASH. MSc thesis. Delft University of Technology. Submitted for graduation in January 2018.

- Goda, Y. *Random Seas and Design of Maritime Structures*; University of Tokyo Press: Tokyo, Japan, 1985. ISBN:4130681109.
- Goseberg, N.; Wurpts, A.; Schlurmann, T., 2013. Laboratory-scale generation of tsunami and long waves. *Coast. Eng.* 79, 57–74
- Hanzawa, M.; Matsumoto, A.; Tanaka, H., 2012. Stability of Wave-dissipating concrete blocks of detached breakwaters against Tsunami. In *Proceedings of the 33rd International Conference on Coastal Engineering*, Santander, Spain, 1–6 July 2012.
- Hunt-Raby, A.; Borthwick, A.G.L.; Stansby, P.K.; Taylor, P.H., 2011 Experimental measurement of focused wave group and solitary wave overtopping. *J. Hydraul. Res.*, 49, 450–464.
- Ikeno, M.; Mori, N.; Tanaka, H., 2001 Experimental study on tsunami force and impulsive force by a drifter under breaking bore like Tsunamis. *Coast. Eng. J.* 48, pp. 846–850.
- Ikeno, M.; Tanaka, H., 2003. Experimental study on impulse force of drift body and tsunami running up to land. *Ann. J. Coast. Eng.* 50, 721–725.
- Jayarathne, M.P.R.; Premaratne, B.; Adewale, A.; Mikami, T.; Matsuba, S.; Shibayama, T.; Esteban, M.; Nistor, I., 2016. Failure mechanisms and local scour at coastal structures induced by Tsunami. *Coast. Eng. J.* 58, 1640017.
- Kato, F.; Suwa, Y.; Watanabe, K.; Hatogai, S., 2012. Mechanism of coastal dike failure induced by the Great East Japan Earthquake Tsunami. In *Proceedings of the 33rd International Conference on Coastal Engineering*, Santander, Spain, 1–6 July 2012.
- Latcharote, P.; Suppasri, A.; Hasegawa, N.; Takagi, H.; Imamura, F., 2016. Effect of breakwaters on reduction of fatality ratio during the 2011 Great East Japan Earthquake and Tsunami. *J. Jpn. Soc. Civ. Eng. Ser. B2* 72, 1591–1596.
- Madsen, P.A.; Furhman, D.R.; Schaffer, H.A., 2008. On the solitary wave paradigm for tsunamis. *J. Geophys. Res.* 113, C12012.
- Mikami, T.; Shibayama, T.; Esteban, M.; Matsumaru, R., 2012. Field survey of the 2011 Tohoku Earthquake and tsunami in Miyagi and Fukushima Prefectures. *Coast. Eng. J.* 54, 1250011.
- Mikami, T.; Matsuba, S.; Shibayama, T. 2014. Flow Geometry of Overflowing Tsunamis Around Coastal Dykes, In *Proceedings of the Coastal Engineering Proceedings 2014*, Seoul, Korea, 15–20 June 2014. Available online: [https://journals.tdl.org/icce/index.php/icce/article/view/7615/pdf\\_839](https://journals.tdl.org/icce/index.php/icce/article/view/7615/pdf_839) (accessed on 1 June 2016)
- Mizutani, S.; Imamura, F., 2000. Hydraulic experimental study on wave force of a bore acting on a structure. *Coast. Eng. J.* 47, 946–950
- Nandasena, N.A.K.; Sasaki, Y.; Tanaka, N., 2012. Modelling field observations of the 2011 Great East Japan tsunami: Efficacy of artificial and natural structures on tsunami mitigation. *Coast. Eng.* 2012, 67, 1–13.
- Mori, N.; Takahashi, T. The 2011 Tohoku Earthquake Tsunami Joint Survey Group, 2012 Nationwide post event survey and analysis of the 2011 Tohoku Earthquake Tsunami. *Coast. Eng. J.*, 54, 1250001.
- Okumura, N.; Jonkman, S.; Esteban, M.; Hofland, B.; Shibayama, T., 2017. A method for Tsunami risk assessment A case study for Kamakura, Japan. *Nat. Hazards* 88, 1451–1472, doi:10.1007/s11069-017-2928-x.
- Ratnayakage, S., Sasaki, J., Esteban, M. and Matsuda, H. 2017. Assessment of the Co-Benefits of Structures in Coastal Areas for Tsunami Mitigation and Improving Community Resilience in Sri Lanka. *International Journal of Disaster Risk Reduction* 23, 80-92
- San Carlos-Arce, R.; Onuki, M.; Esteban, M.; Shibayama, T., 2017. Risk awareness and intended tsunami evacuation behaviour of international tourists in Kamakura City, Japan. *Int. J. Disaster Risk Reduct.* 23, 178–192.
- Sakakiyama, T., 2012. Stability of armour units of rubble mound breakwater against Tsunamis. In *Proceedings of the 33rd International Conference on Coastal Engineering*, Santander, Spain, 30 June–5 July 2012.
- Shibayama, T.; Esteban, M.; Nistor, I.; Takagi, H.; Danh Thao, N.; Matsumaru, R.; Mikami, T.; Aranguiz, R.; Jayaratne, R.; Ohira, K., 2013. Classification of tsunami and evacuation areas. *J. Nat. Hazards*, 67, 365–386.
- Stansby, P.; Xu, R.; Rogers, B.D.; Hunt-Raby, A.; Borthwick, A.G.L.; Taylor, P.H., 2008. Modelling overtopping of a sea defence by shallow-water Boussinesq, VOF and SPH methods. In *Flood Risk Management: Research and Practice*; Samuels P., Huntington S., Allsop W., Harrop J., Eds.; CRC Press: Boca Raton, FL, USA, 2008.
- Tanimoto, K.; Furakawa, K.; Nakamura, H., 1996. Hydraulic resistant force and sliding distance model at sliding of a vertical caisson. In *Proceedings of the International Conference on Coastal Engineering*, Orlando Florida USA, 2-6 September, 1996; PP. 846–850. (In Japanese)
- Tanimoto, L.; Tsuruya, K.; Nakano, S., 1984 Tsunami force of Nihonkai-Chubu Earthquake in 1983 and cause of revetment damage. In *Proceedings of the 31st Japanese Conference on Coastal Engineering*, Tokyo, Japan, 13-14 April 1984.
- Tomita, T., Yeom, G. S., Oyugai, M., Niwa, T., 2012. Breakwater effects on tsunami inundation reduction in the 2011 off the Pacific coast of Tohoku Earthquake. *J. JSCE Ser. B2* 68, 156–60. [https://www.jstage.jst.go.jp/article/kaigan/68/2/68\\_I\\_156/\\_article](https://www.jstage.jst.go.jp/article/kaigan/68/2/68_I_156/_article) (accessed 20 November 2017)
- Takabatake, T.; Shibayama, T.; Esteban, M.; Ishii, H.; Hamano, G., 2017. Simulated Tsunami evacuation behaviour of local residents and visitors in Kamakura, Japan. *Int. J. Disaster Risk Reduct.* 23, 1–14.
- Takagi, H.; Bricker, J., 2014. Assessment of the effectiveness of general breakwaters in reducing tsunami inundation in Ishinomaki. *Coast. Eng. J.* 56, 21.